



ELSEVIER

Thermochimica Acta 320 (1998) 245–252

thermochimica  
acta

## The dehydroxylation of basic aluminum sulfate: An infrared emission spectroscopic study

J.T. Kloprogge\*, R.L. Frost

Centre for Instrumental and Developmental Chemistry, Queensland University of Technology, 2 George Street, GPO Box 2434,  
Brisbane Q 4001, Australia

Received 16 March 1998; received in revised form 15 June 1998; accepted 30 June 1998

### Abstract

The tridecameric aluminum polymer  $[\text{AlO}_4\text{Al}_{12}(\text{OH})_{24}(\text{H}_2\text{O})_{12}]^{7+}$  was prepared by forced hydrolysis of  $\text{Al}^{3+}$  up to an OH/Al molar ratio of 2.2. Upon addition of sulfate, the tridecamer crystallized as the monoclinic basic aluminum sulfate  $\text{Na}_{0.1}[\text{AlO}_4\text{Al}_{12}(\text{OH})_{24}(\text{H}_2\text{O})_{12}](\text{SO}_4)_{3.55}$ . The dehydroxylation of the basic aluminum sulfate has been studied by Fourier transform in-situ infrared emission spectroscopy over a temperature range of 200° to 750°C at 50°C intervals. The spectrum is characterized by the sulfate  $\nu_1$  ( $1024\text{ cm}^{-1}$ ),  $\nu_3$  doublet ( $1117$  and  $1168\text{ cm}^{-1}$ ) and the  $\nu_4$  doublet ( $568$  and  $611\text{ cm}^{-1}$ ) modes. Furthermore, minor bands assigned to nitrate are observed. Upon heating from  $\approx 350^\circ$  to  $400^\circ\text{C}$  major changes are observed, especially in the bandwidth and band intensities. The bands in the hydroxyl stretching region due to the  $\text{Al}_{13}$  group disappear, whereas the bands around  $1050\text{ cm}^{-1}$  display various changes in bandwidths, intensities and positions associated with the dehydration and dehydroxylation of the basic sulfate and the changing of the structure into an aluminum oxosulfate. The nitrate bands diminish upon heating. © 1998 Elsevier Science B.V.

**Keywords:**  $\text{Al}_{13}$ ; Basic aluminum sulfate; Dehydroxylation; Infrared emission spectroscopy; Tridecamer

### 1. Introduction

Forced hydrolysis of aluminum solutions by the addition of base solutions, or homogeneous hydrolysis by the decomposition of urea, is known to result in the formation of a large number of complexes. One of the most studied complexes is the tridecameric complex or  $\text{Al}_{13}$ ,  $[\text{AlO}_4\text{Al}_{12}(\text{OH})_{24}(\text{H}_2\text{O})_{12}]^{7+}$  [1–3]. This tridecamer can be visualized as a central tetrahedral  $\text{AlO}_4$ , surrounded by 12 aluminum octahedrals in the form of a cage. Besides the use of this polymer

in the preparation of pillared clays molecular sieves and heterogeneous catalysts [4–8], it has also commercial value because of its antiperspirant activity and its ability to control the viscosity of kaolinite clay [9].

Johansson [10–12] and Johansson et al. [13] were the first who described the precipitation of two different basic aluminum sulfates, both containing the tridecameric aluminum building unit linked by hydrogen bonding to the oxygen atoms of the sulfate groups. The sodium-containing aluminum sulfate crystallized in the cubic system, whereas the sodium-free sulfate crystallized in the monoclinic system.

In more recent papers, Kloprogge et al. [14,15] described the precipitation of monoclinic basic aluminum sulfate with a small amount of sodium.

\*Corresponding author. Tel.: +61 7 3864 1220; fax: +61 7 3864 1804; e-mail: t.kloprogge@qut.edu.au

Based on their chemical analyses by ICP-AES, they reported a chemical composition per unit cell of  $\text{Na}_{0.1}[\text{AlO}_4\text{Al}_{12}(\text{OH})_{24}(\text{H}_2\text{O})_{12}](\text{SO}_4)_{3.55}\cdot 9\text{H}_2\text{O}$ .  $^{27}\text{Al}$  solid-state magic-angle spinning nuclear magnetic resonance spectroscopy showed that the tridecameric units were still present in the crystal structure. Thermogravimetric analyses indicated that the structure is completely stable up to  $80^\circ\text{C}$ , although 9 mol of physically adsorbed water were lost. Between  $80^\circ$  and  $360^\circ\text{C}$ , the aluminum sulfate crystal gradually decomposed, losing its 12 water and 24 hydroxyl groups. At this stage the aluminum sulfate became X-ray amorphous. Between  $360^\circ$  and  $950^\circ\text{C}$ , with a maximum between  $880^\circ$  and  $950^\circ\text{C}$ , the  $\text{SO}_3$  groups are removed, leaving the aluminum oxide.

The aim of this paper is to describe the thermal degradation of monoclinic basic aluminum sulfate by using a relatively scarcely used technique known as infrared emission spectroscopy (IES) [16–19]. The major advantages of IES are that the discrete vibrational frequencies emitted by thermally excited molecules are measured, in situ, on samples at elevated temperatures. This technique overcomes the problems associated with the use of normal infrared spectroscopic techniques like the use of pressed KBr tablets. Furthermore, it removes the difficulty of heating the sample to a specific temperature followed by quenching before any measurements can be performed, while assuming that no phase changes occur upon cooling. IES actually measures the spectra while the dehydroxylation reactions in the aluminum sulfate are in progress.

## 2. Experimental techniques

### 2.1. Basic aluminum sulfate

The synthesis and characterization of the monoclinic basic aluminum sulfate, used in this study, have been extensively studied by Klopogge et al. [2,14,15]. The tridecameric aluminum polymer was obtained by forced hydrolysis of a 0.5 M aluminum nitrate solution with a 0.5 M sodium hydroxide solution until an OH/Al molar ratio of 2.2 was reached. Next, the basic aluminum sulfate was precipitated by the addition of the appropriate amount of 0.5 M sodium sulfate and aged for 42 days before removal from the solution.

Crystals collected from the wall of the container were shown to be phase pure.

### 2.2. Infrared emission spectroscopy

FT-IR emission spectroscopy was carried out on a Digilab FTS-60A spectrometer, which was modified by replacing the IR source with an emission cell. A description of the cell and principles of the emission experiment have already been published elsewhere [16].

Approximately 0.2 mg of the basic aluminum sulfate was spread as a thin layer on a 6-mm diameter platinum surface and held in an inert atmosphere within a nitrogen-purged cell during heating. The infrared emission cell consists of a modified atomic

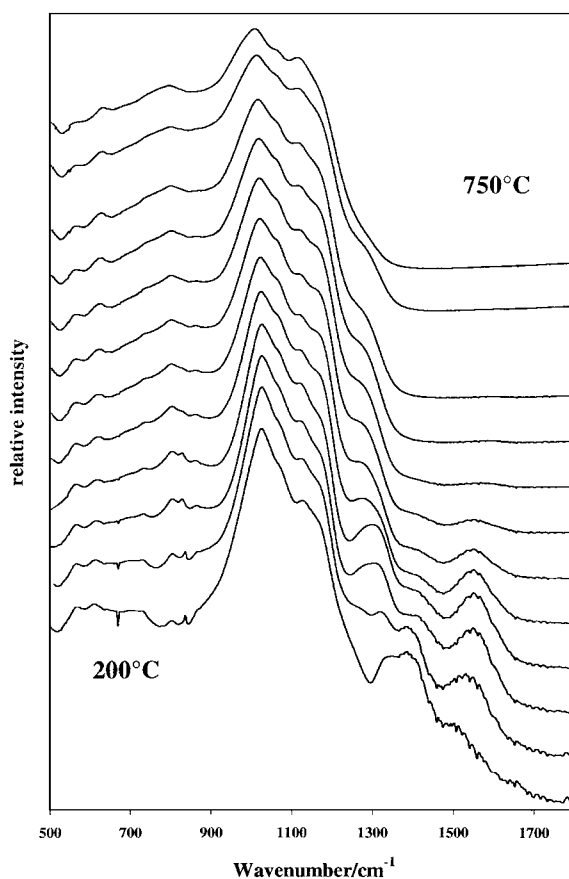


Fig. 1. The infrared emission spectra of basic aluminum sulfate over the  $500$  to  $1800\text{ cm}^{-1}$  range and from  $200^\circ$  to  $750^\circ\text{C}$  at  $50^\circ\text{C}$  intervals.

absorption graphite rod furnace, which is driven by a thyristor-controlled AC power supply capable of delivering up to 150 A at 12 V. A platinum disk acts as a hot plate to heat the basic aluminum sulfate sample and is placed on the graphite rod. An insulated 125- $\mu\text{m}$  type R thermocouple was embedded inside the platinum plate in such a way that the thermocouple junction was  $<0.2$  mm below the surface of the platinum. Temperature control of  $\pm 2^\circ\text{C}$  at the operating temperature of the aluminum sulfate sample was achieved by using a Eurotherm Model 808 proportional temperature controller, coupled to the thermocouple.

The design of the IES facility is based on an off-axis paraboloid mirror with a focal length of 25 mm mounted above the heater which captures the infrared radiation and directs the radiation into the spectrometer. The assembly of the heating block and platinum hot plate is located such that the surface of the platinum is slightly above the focal point of the off-axis paraboloid mirror. By this means, the geometry is such that  $\approx 3$ -mm diameter area is sampled by the spectrometer. The spectrometer was modified by the removal of the source assembly and mounting a gold-coated mirror, which was drilled through the center to allow the passage of the laser beam. The mirror was

mounted at  $45^\circ$ , which enables the IR radiation to be directed into the FT-IR spectrometer.

In the normal course of events, three sets of spectra are obtained: firstly, the black-body radiation over the temperature range selected at the various temperatures; secondly, the platinum plate radiation is obtained at the same temperatures; and, thirdly, the spectra from the platinum plate covered with the sample. Normally, only one set of black-body and platinum radiations is required. The emittance spectrum at a particular temperature was calculated by subtraction of the single-beam spectrum of the platinum back-plate from that of the platinum+sample, and the result ratioed to the single-beam spectrum of an approximate black body (graphite). This spectral manipulation is carried out after all the spectral data has been collected.

The emission spectra were collected at intervals of  $50^\circ\text{C}$  over the  $200$ – $750^\circ\text{C}$  range. The period between scans (while the temperature was raised to the next hold point) was  $\approx 100$  s. It was considered that this was sufficient time for the heating block and the powdered sample to reach a temperature equilibrium. The spectra were acquired by co-addition of 64 scans for the whole temperature range (approximate scanning time 45 s), with a nominal resolution of  $4\text{ cm}^{-1}$ .

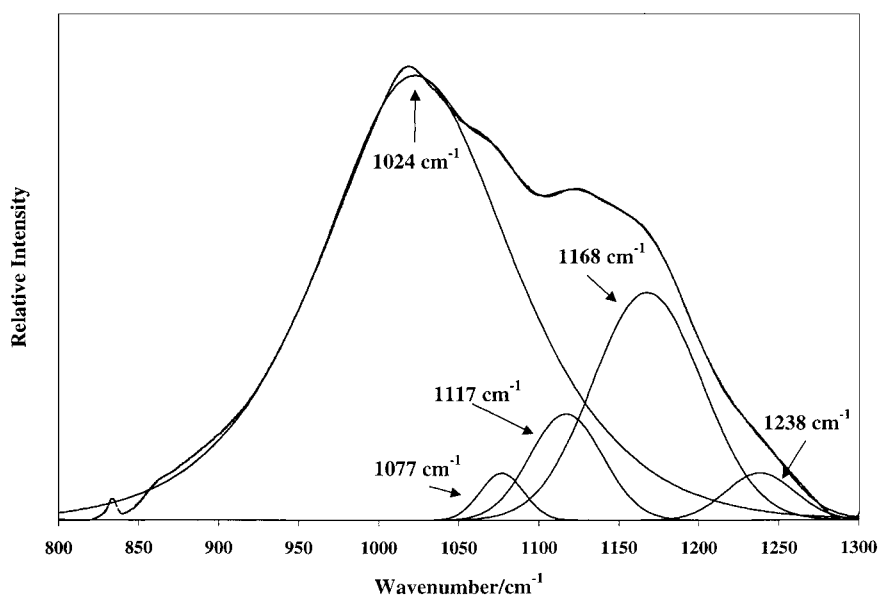


Fig. 2. Band-component analysis of the IES spectrum of basic aluminum sulfate at  $200^\circ\text{C}$  in the  $800$ – $1300\text{ cm}^{-1}$  region.

Good quality spectra can be obtained providing the sample thickness is not too large. If too large a sample is used, then the spectra become difficult to interpret because of the presence of combination and overtone bands. Spectral manipulation such as baseline adjustment, smoothing and normalization was performed using the Spectralcalc software package (Galactic Industries, NH). Band-component analysis was undertaken using the Jandel 'Peakfit' software package which enabled the type of fitting function to be selected and allows specific parameters to be fixed or varied accordingly. Band fitting was done using a Lorentz–Gauss cross-product function with the minimum number of component bands used for the fitting process. The Gauss–Lorentz ratio was maintained at values  $>0.7$  and fitting was undertaken until reproducible results were obtained with squared correlations of  $r^2 > 0.995$ .

### 3. Results and discussion

The emission spectra of the basic aluminum sulfate in the  $500\text{--}1800\text{ cm}^{-1}$  region obtained at  $50^\circ\text{C}$  intervals from  $200^\circ$  to  $750^\circ\text{C}$  are shown in Fig. 1. The  $200^\circ\text{C}$  spectrum at the bottom of Fig. 1 clearly shows a broad complex band around  $1100\text{ cm}^{-1}$  with recognizable bands at  $1168$  (shoulder),  $1117$ ,  $1077$  and  $1024\text{ cm}^{-1}$  with a very weak second shoulder at  $1238\text{ cm}^{-1}$  based on band-component analysis (Fig. 2). A broad band at  $1350\text{ cm}^{-1}$  seems to be made up of two different bands at  $1331$  and  $1386\text{ cm}^{-1}$ , respectively. Another band is observed at  $1502\text{ cm}^{-1}$ . The absence of a water band around  $1635\text{ cm}^{-1}$  is noteworthy, as it was expected based on the initial crystal composition containing nine water molecules. However, the heating to  $200^\circ\text{C}$  seems to be enough to remove all crystal water in agreement with the TGA data indicating dehydration to take place below  $80^\circ\text{C}$  [14].

The band at  $1502\text{ cm}^{-1}$ , while increasing in intensity, shifts  $\approx 35\text{ cm}^{-1}$  towards higher wave numbers (red shift) during heating to  $400^\circ\text{C}$ . At  $550^\circ\text{C}$ , this band disappeared altogether along with the  $1386\text{ cm}^{-1}$  band. Also, the minor bands, visible at  $867$ ,  $834$  and  $731\text{ cm}^{-1}$ , disappear upon heating to  $550^\circ\text{C}$ . These bands are interpreted as belonging to a minor amount of nitrate in the crystal structure of the basic alumi-

num, which was also proven in a recent Raman microscopy study of this material [20], although the amount of nitrate was too small to be detected in the chemical analyses reported earlier by Klopogge et al. [14].

In the lower frequency region, three more bands are visible at  $801$ ,  $611$  and  $568\text{ cm}^{-1}$ . Although the band at  $801\text{ cm}^{-1}$  shifts towards  $782\text{ cm}^{-1}$  upon heating, it still remains visible at  $750^\circ\text{C}$ . The two bands at  $611$  and  $568\text{ cm}^{-1}$  are interpreted as the  $\Delta\nu_4$  doublet of the sulfate, comparable to the  $640$  and  $620\text{ cm}^{-1}$  doublet of sodium sulfate. The  $\Delta\nu_4$  of  $43\text{ cm}^{-1}$  is larger than the  $\Delta\nu_4$  of the sodium sulfate and is more comparable with the  $\Delta\nu_4$  of  $39\text{ cm}^{-1}$ , known for aluminum sulfate [21].

Upon heating, the shoulder at  $1257\text{ cm}^{-1}$  becomes more clearly visible in the  $250^\circ\text{C}$  spectrum, whereas the  $1331\text{ cm}^{-1}$  band shifts to  $1315\text{ cm}^{-1}$ . Further heating to  $300^\circ\text{C}$  results in a combining of both bands

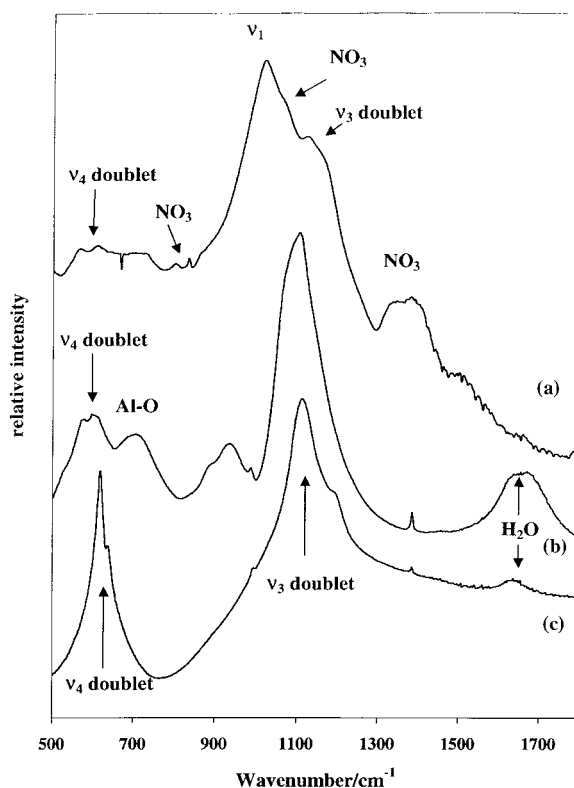


Fig. 3. (a) The infrared emission spectrum of basic aluminum sulfate, and the IR absorption spectra of (b)  $\text{Al}_2(\text{SO}_4)_3 \cdot x\text{H}_2\text{O}$  and (c)  $\text{Na}_2\text{SO}_4 \cdot x\text{H}_2\text{O}$  over the  $500\text{--}1800\text{ cm}^{-1}$  range.

into a new broad band at  $1281\text{ cm}^{-1}$ , which remains visible as a shoulder up to  $750^\circ\text{C}$ . Based upon comparison with hydrated aluminum- and sodium sulfate (Fig. 3), these bands are interpreted as the non-degenerate  $\nu_1$  or else as the triplet  $\nu_3$  of the sulfate group [22], although the  $\nu_3$  is normally observed as a doublet [23], or the doublet  $\nu_3$  of the sulfate group together with a nitrate band at  $1077\text{ cm}^{-1}$ . Based on a comparison with the Raman spectrum, which shows a sharp band at  $1067\text{ cm}^{-1}$  of this basic aluminum sulfate and the fact that normally a doublet is observed, the last option is preferred [20]. The band component analysis of the final product after heating to  $750^\circ\text{C}$  is shown in Fig. 4. Two major bands can be distinguished at  $\approx 994$  and  $1133\text{ cm}^{-1}$ , belonging to the  $\nu_1$  and  $\nu_3$  of the sulfate group with three very minor bands at  $1054$ ,  $1181$  and  $1274\text{ cm}^{-1}$  with relative band intensities of 0.2, 1.0 and 0.4%, respectively.

Thermogravimetric analysis has shown that the basic aluminum sulfate dehydrates and dehydroxylates below  $350^\circ\text{C}$  [14]. This is also reflected in the changes, below  $400^\circ\text{C}$ , in position, bandwidth and relative band intensity as visualized in Fig. 5. The two bands at  $1024$  and  $1077\text{ cm}^{-1}$  reveal a blue shift of 23 and  $30\text{ cm}^{-1}$  over the temperature range from  $200^\circ\text{C}$  to  $750^\circ\text{C}$ , while the two bands at  $1117$  and

$1168\text{ cm}^{-1}$  show a red shift of 16 and  $13\text{ cm}^{-1}$ , respectively (Fig. 5(a)). The bandwidths of the  $1024$  and  $1168\text{ cm}^{-1}$  bands show a strong decrease in width up to  $350^\circ\text{C}$ , indicating that the sulfate positions in the crystal structure become better defined upon dehydroxylation, even though heating stage X-ray diffraction has shown that the dehydroxylated basic aluminum sulfate becomes X-ray amorphous [14]. This is probably more strongly reflected in the continuous increase in the bandwidth of the  $1024\text{ cm}^{-1}$  band from  $350^\circ\text{C}$  up to  $700^\circ\text{C}$ . In contrast, the  $1117\text{ cm}^{-1}$  band shows an increase in bandwidth up to  $250^\circ\text{C}$ , remains constant till  $300^\circ\text{C}$  and then shows a continuous increase till  $\approx 500^\circ\text{C}$  (Fig. 5(b)). A similar contrasting behavior can also be observed in the relative band intensities of the  $1024$  and  $1168\text{ cm}^{-1}$  bands, on the one hand, and the  $1117\text{ cm}^{-1}$  band, on the other hand (Fig. 5(c)).

The  $1077\text{ cm}^{-1}$  band reveals an increase in bandwidth till  $300^\circ\text{C}$ , followed by a decrease up to  $450^\circ\text{C}$ . This can be explained by the fact that the nitrate group is lost from the structure in this temperature interval. Upon denitration, the nitrate group first loses its precise coordination within the structure causing the broadening, followed by the removal of the nitrate causing the narrowing when the amount of nitrate

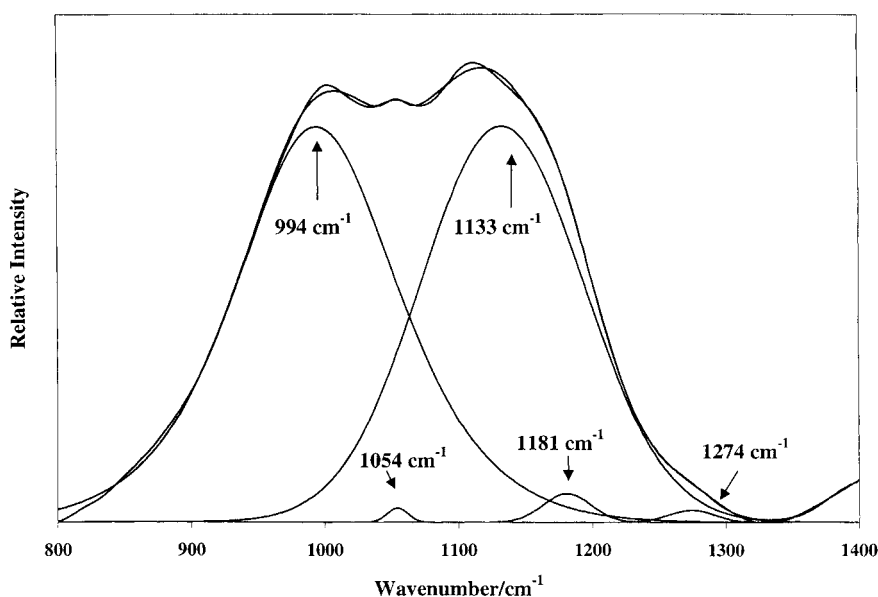


Fig. 4. Band component analysis of the IES spectrum of basic aluminum sulfate at  $750^\circ\text{C}$  in the  $800\text{--}1400\text{ cm}^{-1}$  region.

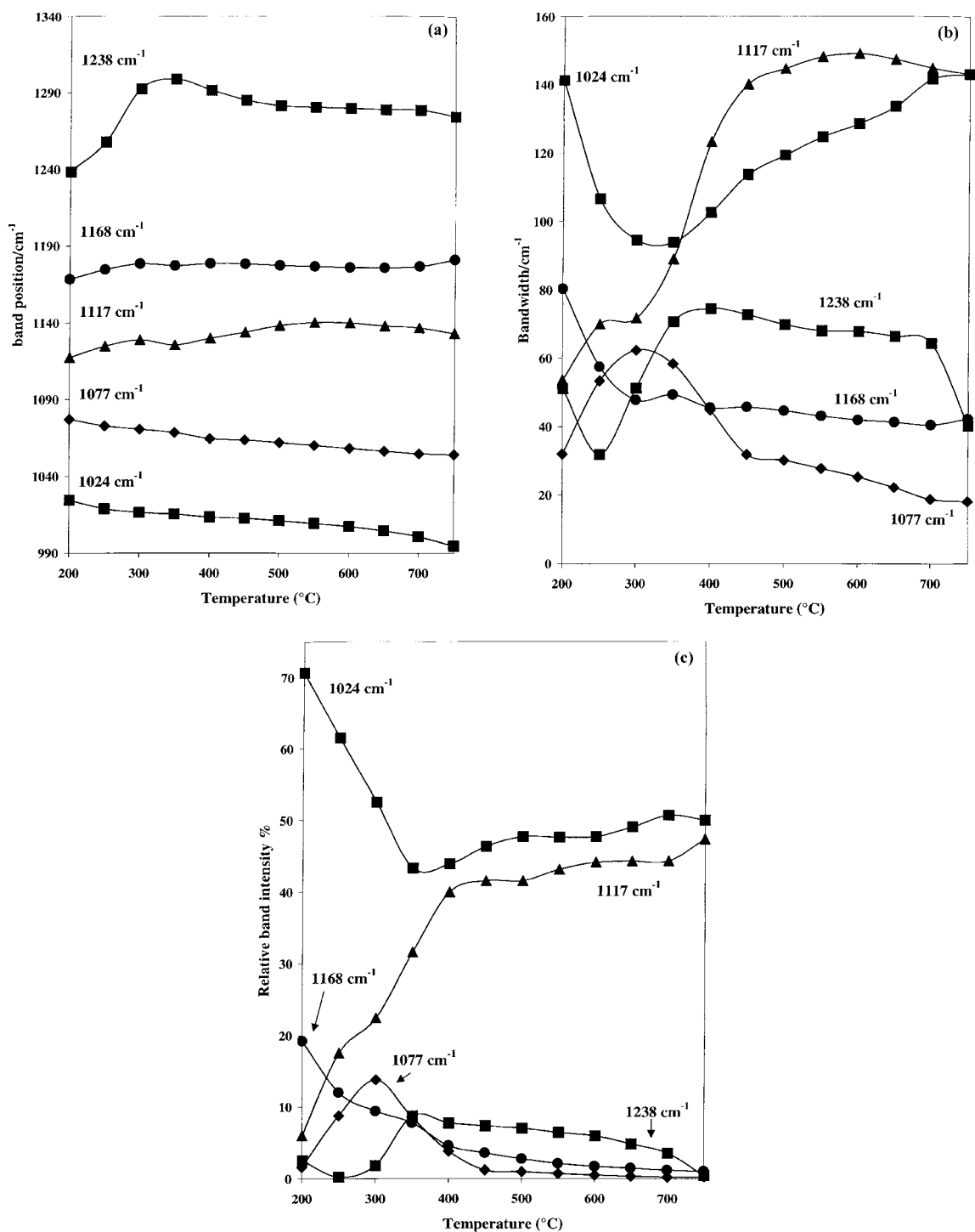


Fig. 5. Changes in the IES (a) band positions, (b) band widths and (c) relative band intensities of the bands in the 1000–1300 cm<sup>-1</sup> region as functions of the temperature.

diminishes. This is also strongly reflected in the relative band intensities, as functions of temperature, of the  $1077\text{ cm}^{-1}$  band.

A very peculiar behavior is shown by the  $1238\text{ cm}^{-1}$  band compared to the other bands in this region between  $1000$  and  $1400\text{ cm}^{-1}$ . First, the band shows a strong red shift of more than  $50\text{ cm}^{-1}$ , followed by a blue shift above  $350^\circ\text{C}$ . The bandwidth reduces to a minimum at  $250^\circ\text{C}$ , followed by an increase till  $350^\circ\text{C}$  after which it remains nearly constant till  $700^\circ\text{C}$ . The relative band intensity shows an opposite behavior. First, it shows an increase till  $250^\circ\text{C}$  followed by a decrease till almost zero at  $450^\circ\text{C}$ . Based on these observations, we suggest that we are looking at changes not of one band but of two different bands. The first band is the band at  $1238\text{ cm}^{-1}$ , which disappears at  $\approx 300\text{--}350^\circ\text{C}$ , and a totally new band develops at higher temperatures, which is attributed to a different structure. Calculations on the mass losses observed in the thermogravimetric analysis by

Kloprogge et al. [14] have suggested that this must be an anhydrous oxosulfate structure with the general formula of  $\text{Al}_{26}\text{O}_{32}(\text{SO}_4)_7$ .

Fig. 6 shows the IES spectra of the hydroxyl-stretching region of the basic aluminum sulfate. Although the lower temperature spectra are rather noisy, a very broad band centred on  $3300\text{ cm}^{-1}$  and a broad band around  $3800\text{ cm}^{-1}$  can be observed. The band around  $3300\text{ cm}^{-1}$  resembles the broad band observed for gibbsite ( $\text{Al}(\text{OH})_3$ ) [24] and is, therefore, interpreted as the hydroxyl stretching modes of the hydroxyl groups present in the Al octahedra. This band disappears after heating to  $\approx 450^\circ\text{C}$ , which is slightly higher than the  $360^\circ\text{C}$  observed in the TGA study [14]. The broad band around  $3800\text{ cm}^{-1}$  disappears after heating to  $300^\circ\text{C}$  and has no known interpretation. Based on the position and the disappearance below  $350^\circ\text{C}$ , it may be suggested that it must be associated with water or hydroxyl groups in the  $\text{Al}_{13}$  structure.

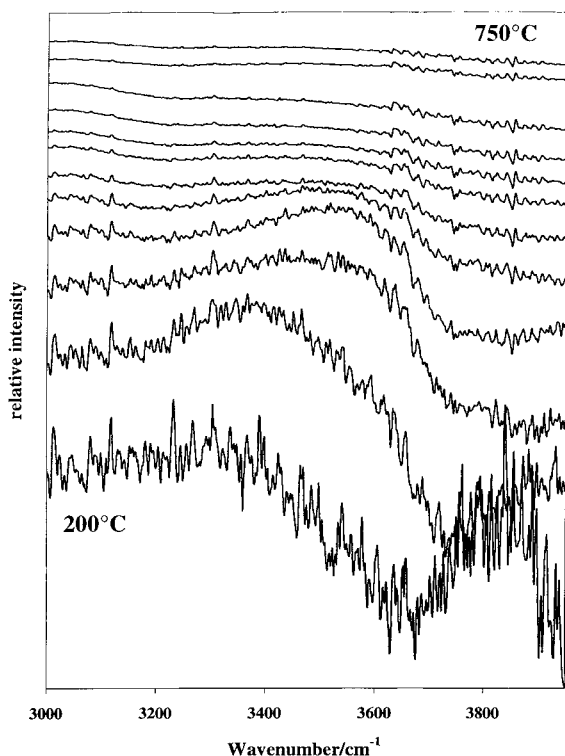


Fig. 6. The infrared emission spectra of basic aluminum sulfate over the  $3000\text{--}4000\text{ cm}^{-1}$  range and from  $200^\circ$  to  $750^\circ\text{C}$  at  $50^\circ\text{C}$  intervals.

## Acknowledgements

The authors thank Greg Cash for his technical assistance with the infrared emission spectrometer. The financial and infra-structural support of the Centre for Instrumental and Developmental Chemistry, the Queensland University of Technology, is gratefully acknowledged.

## References

- [1] J.T. Kloprogge, D. Seykens, J.W. Geus, J.B.H. Jansen, Temperature influence on the  $\text{Al}_{13}$  complex in partially neutralized aluminum solutions: A  $^{27}\text{Al}$  nuclear magnetic resonance study, *J. Non-Cryst. Solids* 142 (1992) 87–93.
- [2] J.T. Kloprogge, D. Seykens, J.B.H. Jansen, J.W. Geus, A  $^{27}\text{Al}$  nuclear magnetic resonance study on the optimization of the development of the  $\text{Al}_{13}$  polymer, *J. Non-Cryst. Solids* 142 (1992) 94–102.
- [3] R.J.M.J. Vogels, Non-hydrothermally synthesized trioctahedral smectites, Ph.D. Thesis, Utrecht University, The Netherlands, Chap. 7, 1996, pp. 157–173.
- [4] D. Plee, L. Gatineau, J.J. Fripiat, Pillaring processes of smectites with and without tetrahedral substitutions, *Clays Clay Miner.* 35 (1987) 81–88.
- [5] A. Schutz, W.E.E. Stone, G. Poncelet, J.J. Fripiat, Preparation and characterization of bidimensional zeolitic structures

- obtained from synthetic beidellite and hydroxy-aluminum solutions, *Clays Clay Miner.* 35 (1987) 251–261.
- [6] J.T. Klopogge, E. Booij, J.B.H. Jansen, J.W. Geus, The effect of thermal treatment on the properties of hydroxy-Al and hydroxy-Ga pillared montmorillonite and beidellite, *Clay Miner.* 29 (1994) 153–167.
- [7] K. Ohtsuka, Preparation and properties of two-dimensional microporous pillared interlayered solids, *Chem. Mater.* 9 (1997) 2039–2050.
- [8] J.T. Klopogge, Synthesis of smectites and porous pillared clay catalysts: A review, *J. Porous Mater.* 5 (1998) 5–41.
- [9] D.L. Teagarden, J.F. Kozlowski, J.L. White, Aluminum chlorohydrate I: Structure studies, *J. Pharm. Sci.* 70 (1981) 758–761.
- [10] G. Johansson, On the crystal structure of some basic aluminum salts, *Acta Chem. Scand.* 14 (1960) 771–773.
- [11] G. Johansson, The crystal structures of  $[Al_2(OH)_2(H_2O)_8](SO_4)_2 \cdot 2H_2O$  and  $[Al_2(OH)_2(H_2O)_8](SeO_4)_2 \cdot 2H_2O$ , *Acta Chem. Scand.* 16 (1962) 403–420.
- [12] G. Johansson, On the crystal structure of the basic aluminum sulfate  $13Al_2O_3 \cdot 6SO_3 \cdot xH_2O$ , *Ark. Kemi* 20 (1963) 321–342.
- [13] G. Johansson, G. Lundgren, L.G. Sillén, R. Söderquist, On the crystal structure of a basic aluminum sulfate and corresponding selenate, *Acta Chem. Scand.* 14 (1960) 769–771.
- [14] J.T. Klopogge, J.W. Geus, J.B.H. Jansen, D. Seykens, Thermal stability of basic aluminum sulfate, *Thermochim. Acta* 209 (1992) 265–276.
- [15] J.T. Klopogge, P.J. Dirken, J.B.H. Jansen, J.W. Geus, One- and two-dimensional  $^{27}Al$  MAS NMR study of basic aluminum sulfate, *J. Non-Crystal. Solids* 181 (1995) 151–156.
- [16] A.M. Vassalo, P.A. Cole-Clarke, L.S.K. Pang, A. Palmisano, Infrared emission spectroscopy of coal minerals and their thermal transformations, *J. Appl. Spectrosc.* 46 (1992) 73–78.
- [17] R.L. Frost, A.M. Vassalo, The dehydroxylation of the kaolinite clay minerals using infrared emission spectroscopy, *Clays Clay Miner.* 44 (1996) 635–651.
- [18] R.L. Frost, Infrared emission spectroscopy and their thermal transformations, in G.J. Churchman, R.W. Fitzpatrick, R.A. Eggleton (Eds.), *Proceedings of the 10th International Clay Conference*. CSIRO Publishing, Melbourne, Australia, 1995, pp. 219–224.
- [19] R.L. Frost, A.M. Vassallo, Fourier transform infrared emission spectroscopy of kaolinite dehydroxylation, *Mikrochim. Acta* 14 (1997) 789–791.
- [20] J.T. Klopogge, R.L. Frost, R. Fry, Raman microscopy study of basic aluminum sulfate, *Proceedings of the 16th International Conference on Raman Spectroscopy*, Cape Town, South Africa, 1998, submitted.
- [21] J.R. Ferraro, *Low-Frequency Vibrations of Inorganic Coordination Compounds*. Plenum Press, New York, 1971, pp. 265.
- [22] H.W. van der Marel, H. Beutelspacher, *Atlas of Infrared Spectroscopy of Clay Minerals and their Admixtures*. Elsevier Amsterdam, 1976, pp. 396.
- [23] S.D. Ross, *Inorganic Infrared and Raman Spectra*. McGraw-Hill, Meadenhead, 1972, pp. 414.
- [24] J.A. Gadsden, *Infrared Spectra of Minerals and Related Inorganic Compounds*. Butterworth. London, 1975, pp. 277.